



Study on the mechanism of destruction triggering of membrane electrode assembly of hydrogen fuel cell

Lei Chen*, Yi-Nan Nie, Hang Yu, Wen-Quan Tao

Key Laboratory of Thermo-Fluid Science and Engineering, Ministry of Education; School of Energy & Power Engineering, Xi'an Jiaotong University, Xi'an, Shaanxi, People's Republic of China, 710049

ARTICLE INFO

Article history:

Received 27 March 2020
Revised 5 June 2020
Accepted 26 June 2020
Available online 9 July 2020

Keywords:

Proton exchange membrane fuel cell
Destruction triggering
Membrane electrode assembly
Microscopic observation

ABSTRACT

In this paper, the mechanism of the destruction triggering of the membrane electrode assembly (MEA) of hydrogen fuel cell is studied. It is proposed that electrochemical destruction is the main cause of MEA failure and the result of other damages. Electron microscopy experiments are carried out on the MEA after 20 h of operation, the MEA after clamping, and the MEA after water immersion freezing, then the trigger role of mechanical destruction and thermal destruction in MEA is revealed. The analysis shows that the mechanical destruction, thermal destruction, electrochemical destruction and the internal mass transfer process of the MEA are coupled to each other to cause MEA destruction. Mechanical and thermal damage play a trigger role in the ultimate destruction and failure of the MEA, which will affect the flow mass transfer process, the flux of the working gasses in the MEA is abnormally increased, resulting in further component destruction and negative electrochemical reaction. Preventing MEA from mechanical and thermal destruction plays a key part of improving its durability. On the one hand, the external clamping should avoid stress points in the MEA area to minimize the external stress. On the other hand, the proton exchange membrane requires lower swelling rate and proper drainage measures in the off state.

© 2020 Elsevier Ltd. All rights reserved.

1. Introduction

In today's energy situation, hydrogen energy is seen as a clean alternative to current mainstream fossil energy. In the utilization of hydrogen energy, hydrogen fuel cell has attracted the attention of scholars because of its high energy density and environmental friendliness [1–6]. The US Department of Energy (DOE) requires a minimum fuel cell life requirement of 5000 h for automotive fuel cells and a life expectancy of at least 40,000 h for distributed generation applications [7]. At present, the life of hydrogen fuel cells is in the range of 3000–5000 h. When the working time exceeds this range, the battery performance drops sharply and cannot be regarded as effective work, which is, the battery fails.

As an important component of the proton exchange membrane fuel cell, the performance of the membrane electrode assembly (MEA) directly affects the working state of the fuel cell. It consists of two gas diffusion layer (GDL), one layer of proton exchange membrane (PEM) and a catalyst layer (CL) sprayed on both sides of the proton exchange membrane (as shown in Fig. 1). The membrane electrode assembly is clamped by a bipolar plate with flow paths during operation. In membrane electrode assembly, hydro-

gen is reduced to protons at the anode, and protons are transported through the proton exchange membrane to react with electrons and oxygen in the cathode to form water. Under the effect of electron proton drag, water is dragged from the anode to the cathode as protons pass. The working process of PEMFC is very complicated, including various physical phenomena such as electrochemical reaction, water transport, proton transfer, gas diffusion, which means multiple physical fields exist in PEMFC, such as electric field, force field and temperature field [7].

The main causes of membrane electrode assembly destruction are electrochemical damage, mechanical damage and thermal damage [8,9]. Factors of chemical destruction include chemical structural degradation of proton exchange membranes, poisoning and migration of platinum catalysts [10–16]. Mechanical damage is caused by mechanical stress caused by the clamping of the external bipolar plate, structural changes caused by working conditions, etc. [17–22]. Thermal damage mainly refers to the degradation of proton exchange membrane sulfonic acid groups at high temperatures due to the activation of platinum particles [23–25].

The fuel cells don't fail in an instant, the failure is a comprehensive result of the combination of multiple damage causes and has some triggering reasons. Also, the three kinds of damage are not parallel, they occur in a certain order and there is a logical relationship. When we talk about the failure of the fuel cell, the

* Corresponding author.

E-mail address: chenlei@mail.xjtu.edu.cn (L. Chen).

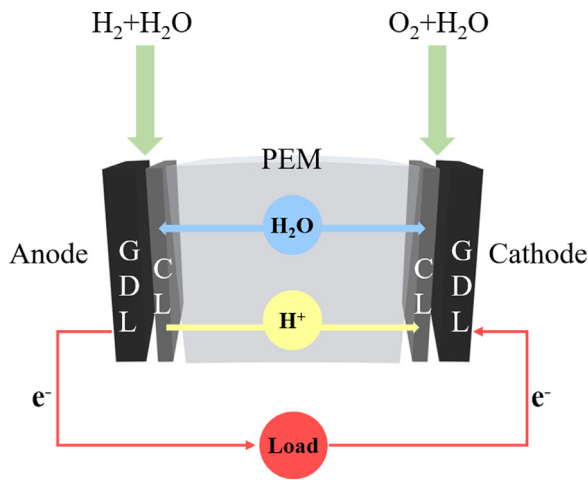


Fig. 1. Proton exchange membrane fuel cell cross section.

exact thing we mean is that the fuel cell cannot perform effective chemical reaction and cannot output the voltage and current value we expect. This illustrates the electrochemical destruction is the last performance of fuel cell, and maybe the results of all kinds of damage, which needs us to prove later.

The researches on the above-mentioned damage situation mostly focus on the discussion of a single failure mechanism, and they correspond to different failure conditions with certain reasons. Akita use analytical TEM to observe Pt particle deposition in PEM and count the penetration depth and agglomeration diameter of platinum particles [25]. And Chen pointed out [14], when platinum particles of catalyst are deposited and agglomerated in PEM, it will cause irregular changes in the water channel, thereby affecting the proton transport capacity of PEM. Uchiyama report the wrinkle deformation of MEA after humidity cycles and point out that preventing MEA buckling can extend PEMFC durability [18]. Yang established a two-dimensional model of a proton exchange membrane fuel cell, pointing out that anode flooding causes hydrogen depletion and carbon corrosion. To a certain extent, the transportation process inside the fuel cell and the destruction of the membrane electrode assembly have been comprehensively considered [13]. Through these studies, a variety of MEA destruction mechanisms have been explained from different perspectives, ~~Although different failure causes can be explained,~~ but there is still a lack of consideration of the overall causes of failure in combination with the operation of the fuel cell. Compared with these studies, this paper pays more attention to how different types of damage together cause the damage of the membrane electrode assembly and the failure of the fuel cell. This includes the different sequences in which different types of damage occur and the logical relationship between them. To be more specific, it is which kind of damage happens first and how does the damage further affects the working process of fuel cells, that we try to find out. Based on this idea, this paper studies the failure trigger mechanism of fuel cell membrane electrode assembly by experimental means, trying to interpret the development process of internal destruction of membrane electrode assembly from a holistic perspective.

2. Experimental methods and equipment

2.1. Experimental equipment apparatus

2.1.1. Proton exchange membrane fuel cell test bench

In this experiment, the fuel cell test platform FCTS50, from Arbin Company of the United States was used. The fuel cell part

of the experimental bench includes reaction gas source supply, gas humidification module, temperature control module and battery temperature control module. The gas supply is supplied by high pressure gas cylinders including hydrogen, air and nitrogen. After the reaction gas passes through the pressure valve, the flow rate is controlled by the mass flow meter, the humidifier adjusts the temperature and humidity of the reaction gas, and then the reaction gas enters the fuel cell through the heat preservation pipeline to react. At last, the reacted gas is discharged to the outside after being dehydrated by the back-pressure valve and the condenser.

2.1.2. Transmission electron microscope (TEM)

In this experiment, JEOL JEM-F200 (HR) field emission transmission electron microscope was used. The dot resolution can reach ≤ 0.23 nm, the lattice resolution can reach ≤ 0.104 nm, the STEM HAADF resolution can reach ≤ 0.19 nm; the highest acceleration voltage is 200 kV, the minimum step size of the accelerating voltage is 50 V; the TEM magnification is 50–6 K times in LOW MAG mode and 1K–2000 K times in MAG mode; STEM magnification is 200–15 K times in LOW MAG mode and 20K–150 M times in MAG mode. Since the membrane electrode assembly is formed by hot pressing of a plurality of layers of materials, wherein the gas diffusion layer and the proton exchange membrane are both porous dielectric materials, the proton exchange membrane requires pretreatment preparation in the following manner: (1) cut a part of the membrane electrode assembly about $2 \text{ mm} \times 10 \text{ mm} \times 0.5 \text{ mm}$, (2) insert the cut membrane electrode assembly into the epoxy resin, (3) re-slicing the resin and put the sample on a copper grid by a carbon microgrid. Then the sample can be sent on the sample rod into the TEM for observations.

2.1.3. Scanning electron microscopy (SEM)

In this experiment, Gemini SEM 500 field emission scanning electron microscope was used. The resolution is 0.6 nm at 15 kV and 0.9 nm at 1 kV (with the option of series deceleration). The accelerating voltage is in the range of 0.02–30 kV. Continuously adjustable, the magnification range is 20–2000 K times, and the probe current is adjustable between 3 pA–20 nA. At the same time, the electron microscope is equipped with an energy spectrum and a super energy spectrometer for elemental analysis. In the scanning electron microscope, it is not necessary to perform excessive pretreatment on the membrane electrode assembly. The membrane electrode assembly is directly cut into a sample of about $5 \text{ mm} \times 10 \text{ mm} \times 0.5 \text{ mm}$, and the conductive paste is vertically attached to the vertical sample stage to facilitate observation of the membrane electrode assembly cross section.

2.2. Experimental methods

2.2.1. Membrane electrode assembly operation experiment

The membrane electrode assembly used in the experiment is prepared by hot pressing of the SFR7201 proton exchange membrane and the TGP-H-060 gas diffusion layer from Asahi Kasei Co., Ltd. The operation experiment was performed using the fuel cell test platform FCTS50 mentioned above. The experimental steps are as follows:

2.2.1.1. Operating conditions stabilization. Battery temperature and dew point humidifier temperature usually require 1–2 h to stabilize. In order to insert the effect of the relative humidity change of the reaction gasses on the MEA conversion state, the reaction gasses are discharged through the bypass without venting into the fuel cell before the dew point temperature stabilizes to the set value. When the dew point temperature is stabilized, the bypass is turned off alternately and the reaction gasses are vented into

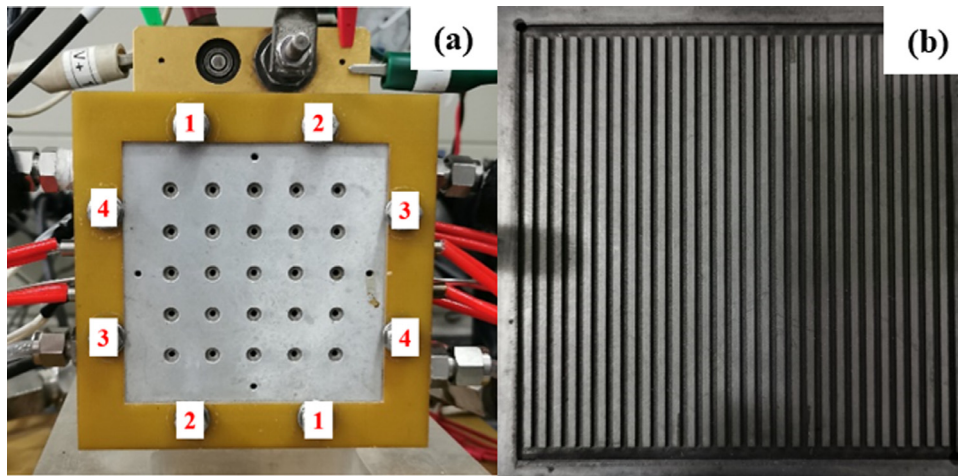


Fig. 2. The standard fixture of the FCTS50 fuel cell test bench (a) and the flow field plate (b).

the fuel cell. At this point, all operating conditions of the fuel cell are stable and reach preset values.

2.2.1.2. Membrane electrode assembly initialization. After the battery operating conditions are stable, in order to eliminate the effects of previous experiments on the membrane electrode assembly state of the battery, the membrane electrode assembly state needs to be initialized. The fuel cell was operated at a current density of $0.4 \text{ A}\cdot\text{m}^{-2}$ for 1 h, so that the membrane electrode assembly was fully wetted, and the effect of the previous operation on the membrane electrode assembly was eliminated.

2.2.1.3. Continuous operation process. After the above two steps, the operating conditions of the battery and the initial state of the membrane electrode assembly have been stabilized, and continuous operation can be performed for a long time. Cycle the current density in the range of $0\text{--}1 \text{ A}\cdot\text{cm}^{-2}$ for a certain period of time, and the current step is $0.1 \text{ A}\cdot\text{cm}^{-2}$. In this paper, the total operating time of the fuel cell is 20 h.

2.2.2. Membrane electrode assembly clamping experiment

In both the experimental process and the actual working process, the main external stress to the membrane electrode assembly is caused by the fixed fixture, which is a necessary measure to ensure that the working gasses do not leak. In order to discuss the influence caused by this external stress, in this paper, the new membrane electrode assembly was clamped for 48 h by using the standard fixture of the FCTS50 fuel cell test bench (as shown in Fig. 2(a)) and then taken out for observation. The fixture is fixed by 8 bolts, which are divided into 4 groups according to the diagonal rule. When tightening the bolts, each group of bolts is first reinforced with a torque of $12 \text{ N}\cdot\text{m}$ and then in the same order at $14 \text{ N}\cdot\text{m}$ and $15 \text{ N}\cdot\text{m}$ for reinforcement. According to the uniform load on the area of $10 \text{ cm} \times 10 \text{ cm}$, the average external pressure is 6.4 MPa. The flow field plate used within the fixture is a parallel flow channel flow field plate as shown in Fig. 2(b).

2.2.3. Membrane electrode assembly freezing experiment after immersion in water

In this paper, the typical situation of the internal icing of the membrane electrode assembly during the cold start of the fuel cell was simulated. The new membrane electrode assembly after weighing was immersed in deionized water for two hours at room temperature ($22 \text{ }^\circ\text{C}$), then taken out and weighed again. After wrapping the moisture in plastic wrap and aluminum foil paper to prevent evaporation, the membrane electrode assembly was frozen

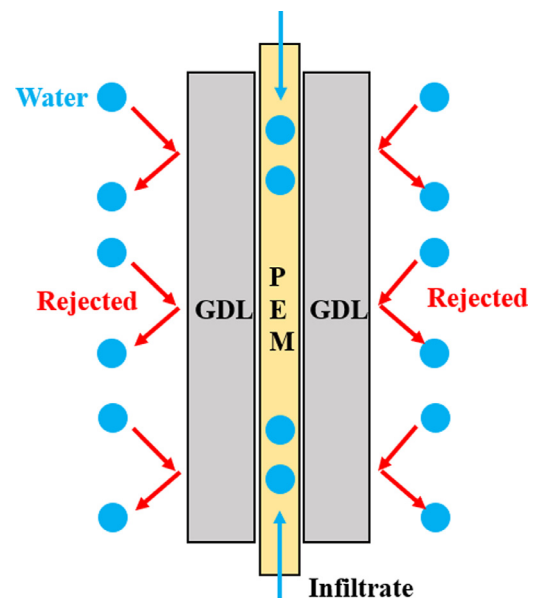


Fig. 3. Schematic diagram of moisture distribution of membrane electrode assembly after immersion in water.

at $-10 \text{ }^\circ\text{C}$ for 48 h, and then dried at room temperature. According to the freezing deformation of water, it can be calculated that the pressure that can be generated inside the membrane electrode assembly can locally reach a maximum of 20 MPa [26].

In the experiment, two membrane electrode assemblies were selected for immersion. Considering that the gas diffusion layer has a certain hydrophobicity [27,28], water does not easily penetrate into the membrane electrode assembly from the gas diffusion layer side, and one of the membrane electrode assemblies was selected to be cut into two halves from the middle trying to increase its water content. It can be seen from Table 1 that the water contents of the three samples are at a low level. Since the whole membrane electrode assembly sample has an uncut partial proton exchange membrane around it, the hydrophilicity of the proton exchange membrane gives it the highest water content. While the cut membrane electrode assembly exposes the cross section to water, the hydrophobicity of the gas diffusion layer blocks the entry of water (as shown in Fig. 3). The whole membrane electrode assembly with the highest water content was selected for scanning electron microscopy experiment.

Table 1
Water content after membrane electrode assembly immersed in water.

	Original weight	Weight after immersion	Water content
Monolithic MEA	1.6155 g	1.7380 g	7.58%
Half block MEA1	1.9231 g	2.0242 g	5.25%
Half block MEA2	1.2200 g	1.249 g	2.38%

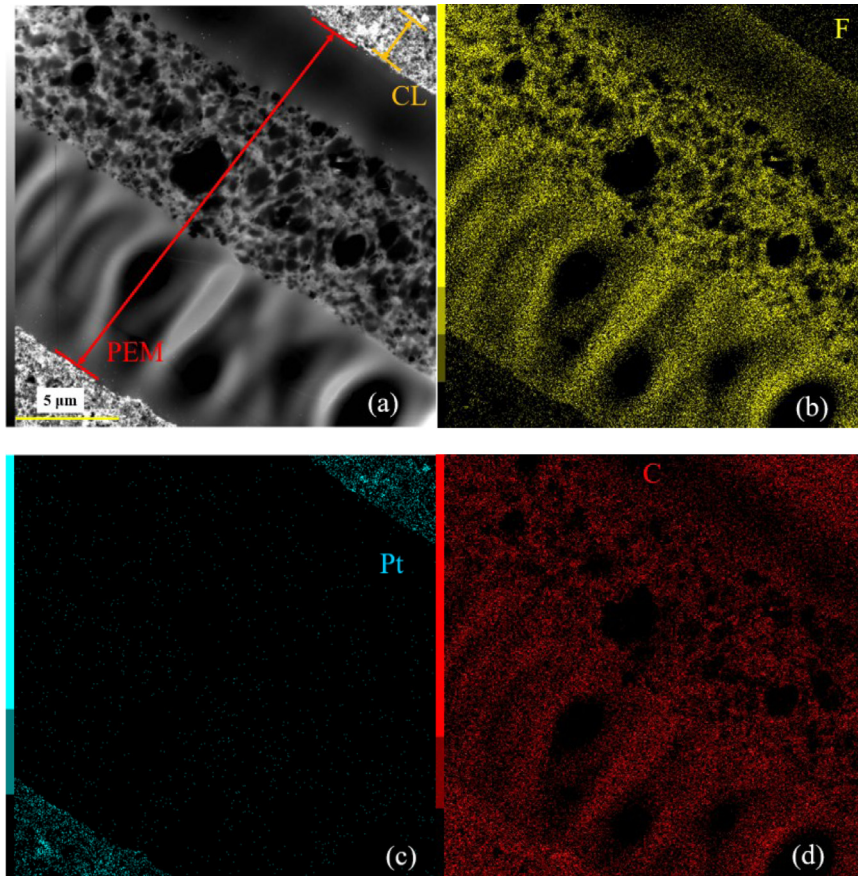


Fig. 4. Transmission electron micrograph and element localization map of proton exchange membrane.

3. Results and discussion

In this paper, we study several kinds of destruction triggering of membrane electrode assembly, most of them are related to mechanical and thermal factors. As mentioned above, we make an assumption that the electrochemical damage is the end result of thermal damage and mechanical damage. In order to prove the above viewpoints, the working stage of the membrane electrode assembly was first judged by the movement of the platinum particles, and then a series of experiments were carried out to analyze the mechanism of mechanical stress and thermal stress triggering of the fuel cell membrane electrode assembly destruction by electron microscopy.

3.1. Movement of platinum particles

Firstly, the cross section of the worked membrane electrode assembly was observed by transmission electron microscopy, and the movement of platinum particles was observed and counted. As mentioned, being different from most existing studies that use a long-term multi-cycle method, we attempt to find out what kind of damage has occurred and what effect it has inside the membrane electrode assembly in the early working state. Since the re-

search in this paper tries to ensure that the observed membrane electrode assembly remains in the early working state, The membrane electrode assembly chosen to be observed in this paper was operated under standard working conditions for 20 h following the steps in section 2.2.1.

In the experimental method section, the TEM preparation steps of the membrane electrode assembly have been described, and the prepared slice is placed in the transmission electron microscope for observation. Since we are focusing on the movement of platinum particles from the catalyst layer to the proton exchange membrane, the observation area was first determined by targeting the proton exchange membrane. Fig. 4(a) shows a direct view of the observation area, while Fig. 4(b)(c)(d) shows the distribution of fluorine, platinum and carbon elements in the observation area.

Through elemental analysis, the components in the observation area are located, the positioning principle is to find the main elements corresponding to the components. Since the inside of the membrane electrode assembly is symmetrically distributed with proton exchange membrane, the position of the proton exchange membrane can be used to substantially determine the membrane electrode assembly distribution within the observation region. As we can tell, only the proton exchange membrane contains a large amount of fluorine in the membrane electrode assembly [25], so

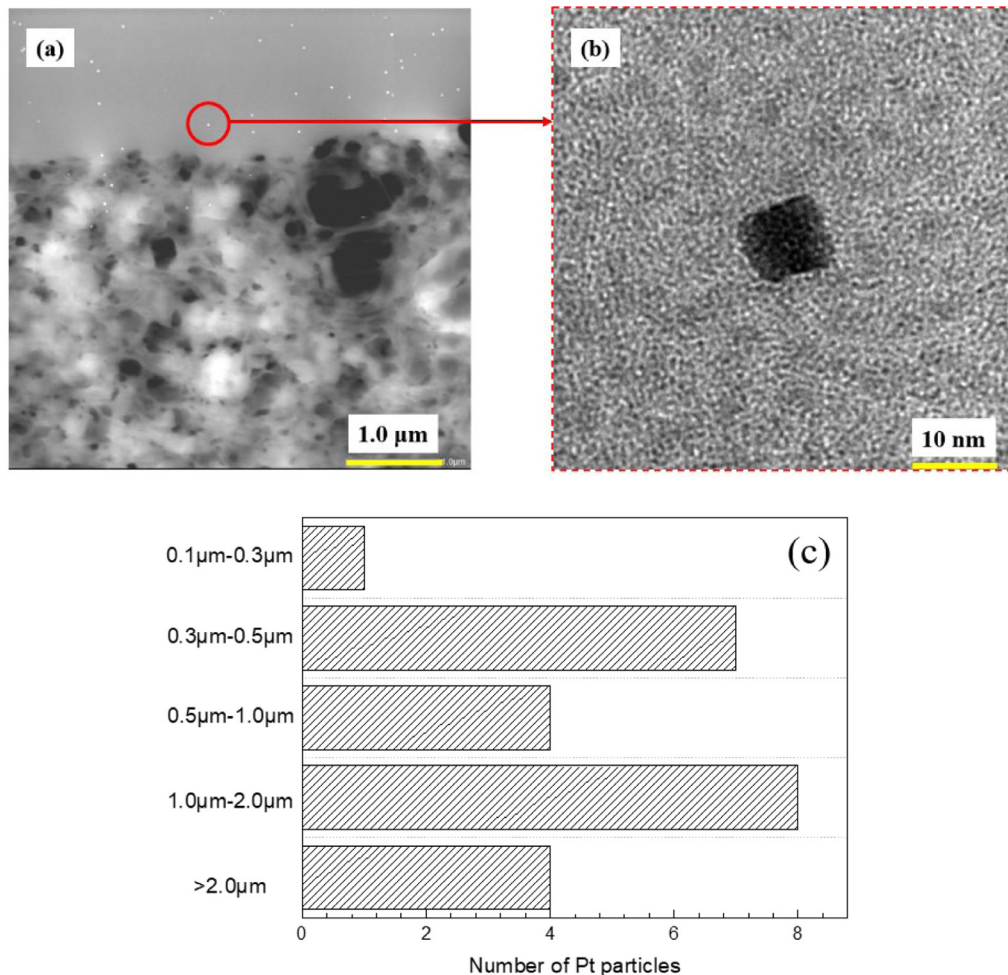


Fig. 5. Schematic diagram of the entry of platinum particles into the proton exchange membrane(a), the diameter of the platinum particle(b) and the depth map(c).

the position of the proton exchange membrane can be located by the distribution of fluorine (as shown in Fig. 4(b)).

As the region of platinum particle motion is from catalyst layer to proton exchange membrane, and the position and boundary of the catalyst layer can be determined by the positioning of platinum elements (as shown in Fig. 4(c)), the location of the observed area is completely determined. As can be seen in Fig. 4(a), the proton exchange membrane has a cotton-like porous structure inside, and the catalyst layer exhibits a high contrast due to the presence of a large amount of platinum particles.

After the observed region is positioned and the components of membrane electrode assembly are figured, attention is now turned to the platinum particle movement in the surrounding area of the proton exchange membrane. In Fig. 5(a), the area below the picture shows the cotton-like shape is the proton exchange membrane, and the upper part of the interface attached with the proton exchange membrane is the transition layer between the catalyst layer and the proton exchange membrane. The bright spots of white in the figure are platinum particles. During the observation, it was found that there was an observable migration of platinum particles in the membrane electrode assembly, and some of the platinum particles entered the proton exchange membrane (as shown in Fig. 5(a)), but the depth of entry was still shallow: 20 of the Pt particles entered a depth of less than $2 \mu\text{m}$, relative to the thickness of the proton exchange membrane of tens of microns (the statistical entry depth of 24 platinum particles in the observation region is shown in Fig. 5(c)).

At the same time, it was found that the diameter of the platinum particles was substantially within 10 nm (as shown in Fig. 5(b)), while Tomoki Akita et al. [25] found that the diameter of platinum particle clusters in the proton exchange membrane is in a range of 50–100 nm after 87 h of accelerated degradation experiments. It indicates that the platinum particles have not been agglomerated. This is because the platinum particles migrate first due to the driving force of the flow mass transfer during the working process, and adhere to the surface of the inside micro-pores after migrating into the proton exchange membrane. The following platinum particles that enter the proton exchange membrane have a chance to bind to the attached platinum particles, and after a period of cumulative growth, they become agglomerated with larger platinum particles. However, the membrane electrode assembly observed here only passed the standard operating condition test for 20 h. At this time, only the initial migration of the platinum particles occurred, and there was no agglomeration, indicating that the fuel cell is still “young” enough to be studied for the damage triggering mechanism, especially for electrochemical damage.

3.2. Mechanical damage of the membrane electrode assembly

In the above experiment of transmission electron microscopy, it is found that the migration and agglomeration of platinum particles are still in the preliminary stage, which indicates that no fatal damage has occurred yet. The completion of electrochemical destruction takes a long time and is not obvious at the beginning of

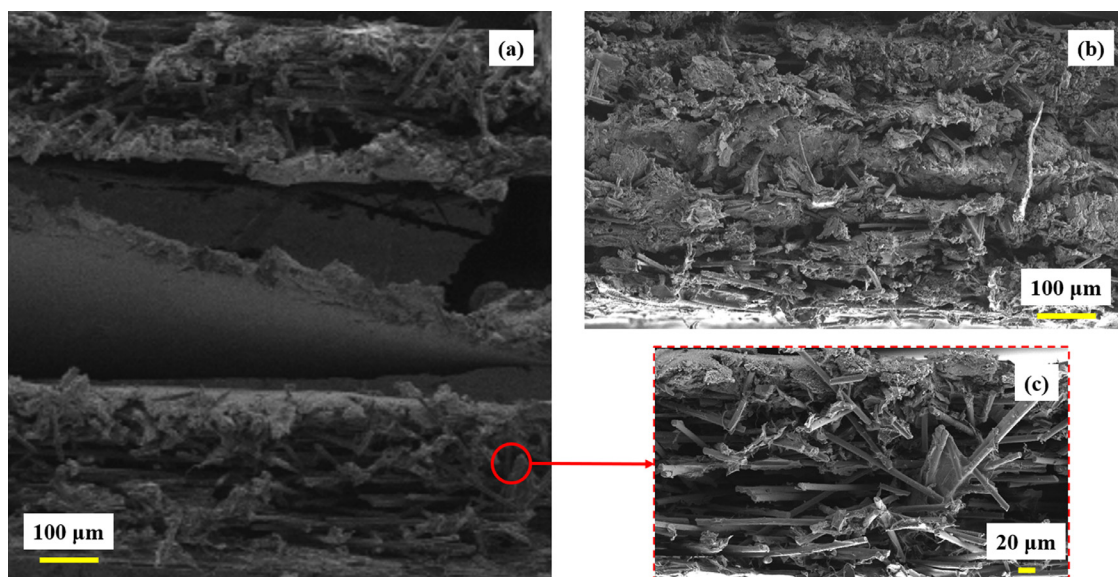


Fig. 6. Comparison of membrane electrode cross sections before work (a) and after work for 20 h.

operation; at the same time, its genesis is complex and involves various reactions. The electrochemical reactions which will be regarded as electrochemical damage are usually caused by the unexpected encounter of the reaction gasses in proton exchange membrane. The little normal cracks in membrane electrode assembly may result in unexpected flow and lead into further electrochemical damage. Compared to the diffusion in the porous media or the permeation through membrane, the reaction gasses flow more easily in the cracks, which can be considered as micro-channels.

To confirm this conjecture, a set of controlled scanning electron microscope observation experiments was performed on the unoperated membrane electrode assembly and the membrane electrode assembly after 20 h of operation. As can be seen in Fig. 6(a), the unoperated membrane electrode assembly shows the basic structural arrangement of the GDL-PEM(CL)-GDL (the catalyst layer is represented as a whole by the proton exchange membrane due to its scale), the outer boundaries of each component are complete and clear. The amplified details of the gas diffusion layer can be seen in Fig. 6(c), the carbon fibers in the gas diffusion layer didn't show massive broken. Fig. 6(a) gives a benchmark of the membrane electrode assembly cross section, there is a clear interface between the gas diffusion layer and the proton exchange membrane, and the membrane electrode assembly shows a distinct multilayer structure.

As can be seen in Fig. 6(b), the cross section of the membrane electrode assembly after working is extremely messy, it is impossible to clearly distinguish the layers of the components, and the overall structure has become loose. At the same time, a large number of the carbon fibers of gas diffusion layers directly inserted into the proton exchange membrane, causing irreversible mechanical damage, the gas diffusion layer is unable to maintain the original structure and the interface with the proton exchange membrane cannot be confirmed. It is precisely because each component has lost its own mechanical rigidity and integrity, as can be seen from the comparison of Fig. 6(a) and Fig. 6(b), the thickness of the membrane electrode assembly after working is only half of the new membrane electrode assembly.

After 20 h of operation, the migration and agglomeration of platinum particles is still in the preliminary stage (stated in chapter 3.1), while the mechanical damage shown in Fig. 6(b) is already very serious. This indicates that the time point of mechanical destruction of the membrane electrode is earlier than that of the

electrochemical reaction. The above-mentioned observed destruction of the component structure and the interface can lead to an increase in gas permeation and a decrease in the proton conductivity of the proton exchange membrane, which confirms the conjecture that the mechanical damage is the main triggering reason of long-term damage and failure.

The membrane electrode assembly is composed of multi-component hot pressing, and the gas diffusion layer and the proton exchange membrane are both porous for the flow and mass transfer. The mechanical damage causes of the membrane electrode assembly can be divided into external stress and internal stress. The external stress is mainly caused by the hot pressing in the production process and fixing in the working process. The internal stress may be performed by internal fluid flow, thermal deformation and other internal forces. The following experiments are carried out from these two aspects to study the intermediate state between the unworked state and the complete mechanical damage.

3.2.1. External stress damage

Membrane electrode assembly subjected to external stress is performed by membrane electrode assembly clamping test in section 2.2.2. It can be visually seen that the edge of the clamped membrane electrode assembly exterior has the same obvious indentation as the shape of the flow field plate, and even causes partial gas diffusion layer to crack (as shown in Fig. 7(a)).

It can be observed in Fig. 7(b) that there is still a distinct layering inside the membrane electrode assembly, but the structure becomes looser than the original structure, and the proton exchange membrane is pressed and attached to the gas diffusion layer on the lower side. It can be observed that the gas diffusion layer is quite clear in the MEA cross section, however, the proton exchange membrane is kind of compressed and fitted to the surface of the gas diffusion layer on the lower side.

At the interface between the gas diffusion layer and the proton exchange membrane, polygonal cracks occurred on the gas diffusion layer side (as shown in Fig. 7(c)), and irregular continuous creep occurred on the proton exchange membrane side (as shown in Fig. 7(d)). This phenomenon reflects the different material properties of gas diffusion layer and proton exchange membrane. The main internal structure of the gas diffusion layer mentioned above is the carbon fiber structure, which exhibits high strength as a whole, while the main component of the proton exchange mem-

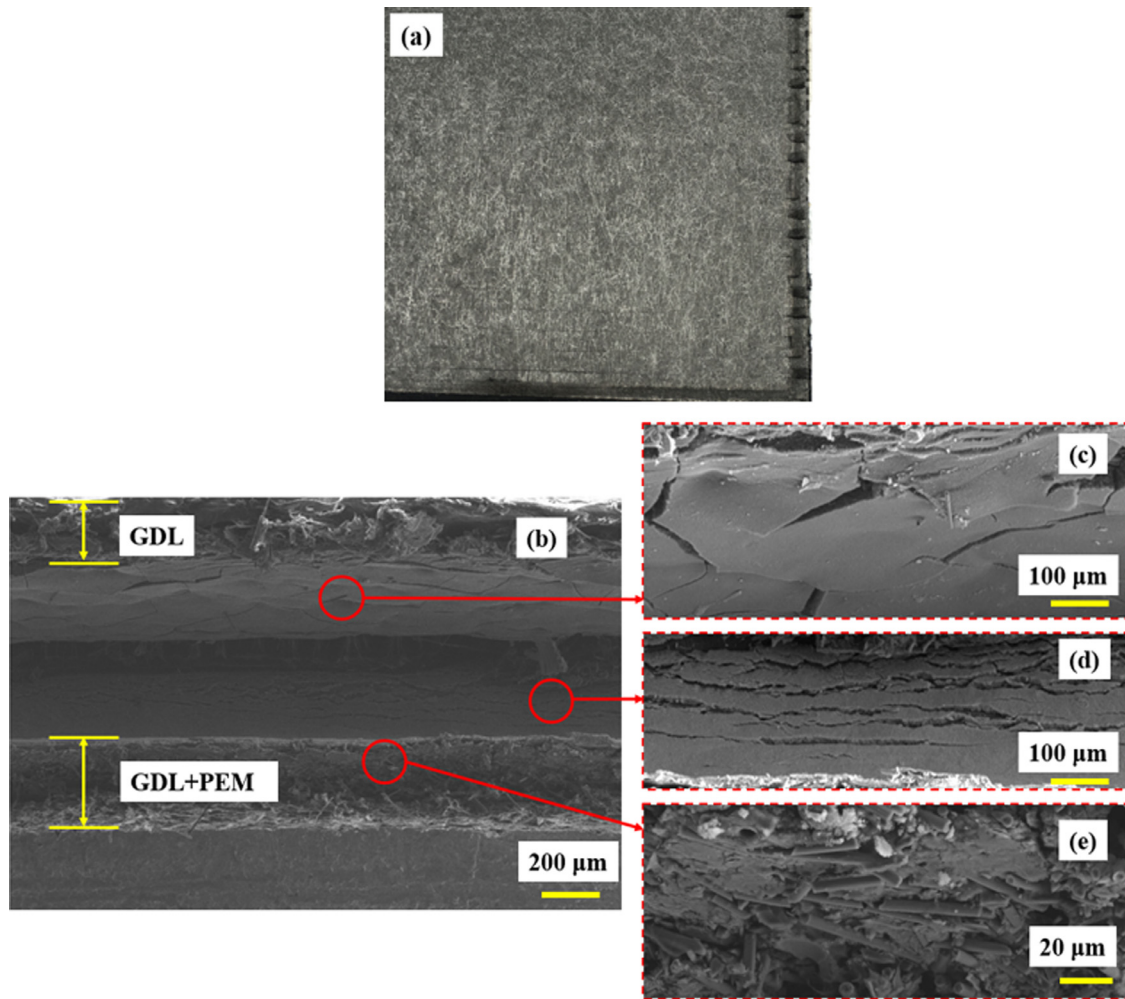


Fig. 7. The appearance and cross-sectional view of the membrane electrode assembly after being clamped.

brane is a polymer with a relatively dense but softer structure. After amplification, it can also be seen that there is a large amount of broken carbon fiber embedded in the proton exchange membrane at the interface (as shown in Fig. 7(e)), but there is still an intuitive difference compared with the case where the carbon fiber inside the membrane electrode assembly is directly inserted into the proton exchange membrane after the operation (as shown in Fig. 6(b)). In general, the components still maintain a good overall shape, and the entire membrane electrode assembly is in a relatively structural balanced state.

3.2.2. Internal stress damage

The frozen membrane electrode assembly in Fig. 8(a) was obviously bent to the sides due to the different thermal expansion coefficients of the components resulting in different deformation ratios. Fig. 8(b) is the scanning electron micrograph of the membrane electrode assembly section after the freezing experiment. When scanning electron microscopy is performed, it can be seen the cut sample can hardly remain integrated status, and the multilayer structure of the membrane electrode assembly has completely lost its tightness and stability. It can be seen from Fig. 8(b) that there is still a relatively obvious delamination inside the membrane electrode assembly, but the deformation of each layer is basically clear. The proton exchange membrane loses its integrity but produces irregular and uneven layered horizontal tears from the inside (as shown in Fig. 8(c)), while there is still a significant physical connection between the layers indicates that the membrane is

not completely torn. At the same time, the carbon fiber arrangement inside the gas diffusion layer remains in a relatively regular state without significant damage (as shown in Fig. 8(d)).

3.3. Different effects of internal and external stress

From the above experimental results, we can find that external stress and internal stress cause two different forms of mechanical damage to the fuel cell membrane electrode assembly. Since the membrane electrode assembly is made by hot pressing of the multilayer component, when the membrane electrode assembly is subjected to external stress, the stress is transmitted and concentrated at the interface between the gas diffusion layer and the proton exchange membrane, then the destruction occurs on both surfaces of the interface. At the same time, due to the high carbon structure strength of the gas diffusion layer, polygonal cracks appear on the surface, and there is also a certain carbon fiber fracture inside. The proton exchange membrane has a low strength and a continuous irregular creep on the surface, which is different from the rigidity of the gas diffusion layer and tends to tear. At the same time, due to the difference in strength between the carbon fiber and the proton exchange membrane, the phenomenon that the fractured carbon fiber shown in Fig. 6(e) is embedded in the surface of the proton exchange membrane is also caused.

When the membrane electrode assembly is immersed in water, the water mainly accumulates in the micro-pores of the proton exchange membrane. After film icing in the micro-pores, the water

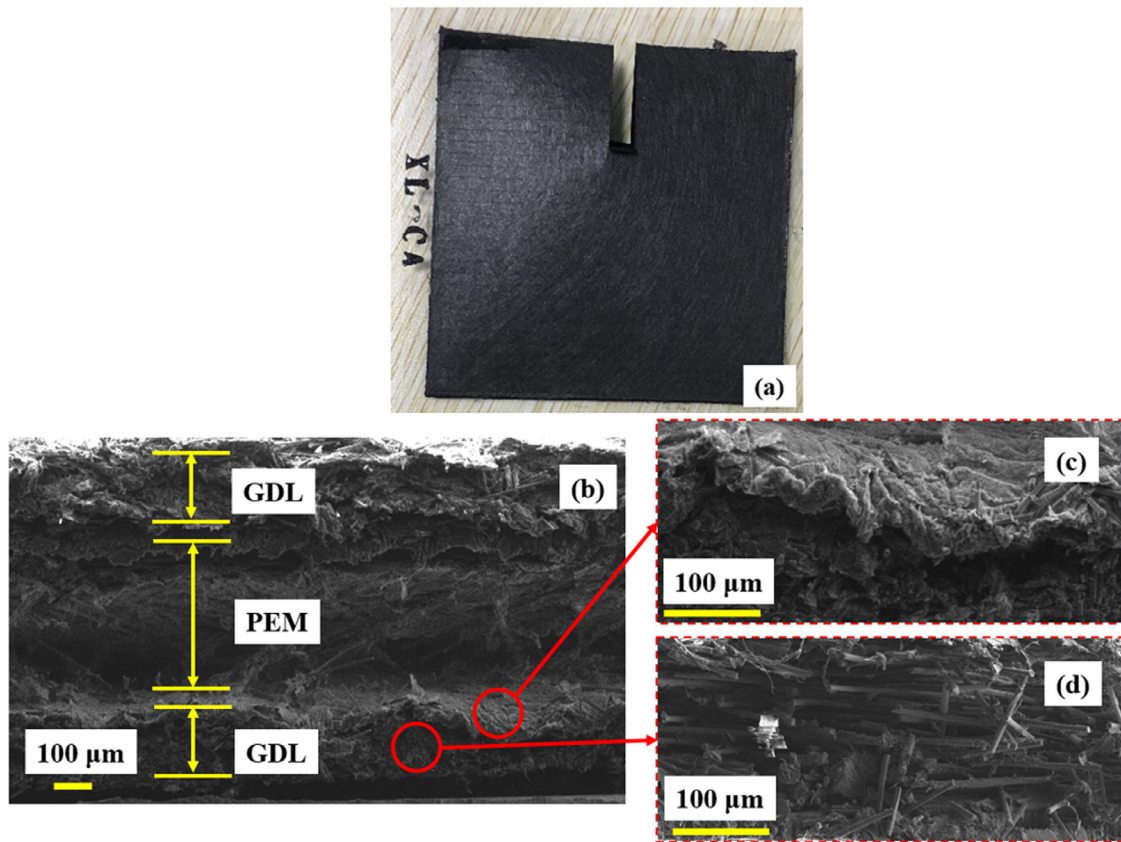


Fig. 8. The appearance and cross-sectional view of the membrane electrode assembly after freezing.

volume expands to generate internal stress, thus producing irregular uneven delamination tear in Fig. 8(c). The tearing phenomenon here is kind of different with the surface tear of the proton exchange membrane caused by external stress. The external stress acts on the surface of the film as a whole, causing cracking in the surface and longitudinal direction. The cracking is mainly related to the fixing of the clamp, and is relatively a static process, which tends to be stable after a certain period of time. The internal stress is caused by the volume change of the local water in the freezing process. It mainly causes tearing in the transverse direction of the membrane, but this process is a dynamic process. There is a possibility of continuous deterioration, the denser and more uniform the local tear occurs, the more severe the membrane will be destroyed.

As the gas diffusion layer is hydrophobic, it is hard to hold a large amount of water inside. And its internal carbon fiber structure has larger pores than proton exchange membrane, the water volume expansion after freezing is not enough to cause obvious damage to its structure, so the carbon fiber remains relatively regular arrangement. In summary, the external stress mainly causes mechanical damage to the internal structure of the gas diffusion layer, the interface of gas diffusion layer and the proton exchange membrane, and the internal stress mainly causes mechanical damage to the internal structure of the proton exchange membrane.

3.4. Dynamic process of membrane electrode assembly destruction

Combined with the analysis of Fig. 5 and the literature research [25], it can be concluded that the migration and agglomeration of platinum particles accumulate with the increase of working time. After 20 h of operation in this paper, the platinum particles in the membrane electrode assembly had only initially migrated, indicat-

ing that electrochemical destruction had not yet occurred. At the same operating time, as shown in Fig. 6(b), the mechanical structure of the membrane electrode assembly was severely damaged. This shows that the mechanical damage occurs before the electrochemical damage, so we make a key discussion on the mechanical damage from the external stress and the internal stress, and analyzed its working principle and subsequent impact on the fuel cell work.

It is worth noting that although external stress and internal stress cause significant mechanical damage to the membrane electrode assembly, the membrane electrode assembly assemblies in Fig. 7 and Fig. 8 maintains a relatively complete shape comparing the membrane electrode assembly cross sections in Fig. 6(b). The components in Fig. 7 and Fig. 8 appear as in clearer stratification and the entire membrane electrode assembly is in a relatively balanced state (the loose structure of the membrane electrode assembly in the freezing experiment is due to the absence of external fixation of the fixture in the experiment). However, the damage of the membrane electrode assembly by static stress provides the basis for the further failure of the membrane electrode assembly.

When the static stress causes the membrane electrode assembly to start mechanical damage, the gas flow and the mass transfer process during the working process will provide a vertical driving force, which will directly destroy the relative equilibrium state of each component, such as the gas diffusion layer and the proton exchange membrane rupture in Fig. 6 (which will form several openings at the originally integral surface). The cracking is further expanded until the interface of gas diffusion layer and proton exchange membrane is broken, (1) the lateral compressive and tensile resistance of each layer are greatly impaired, (2) the flow and mass transfer process will be messed because of the unwanted opening, (3) the working gas (oxygen and hydrogen) enter the pro-

ton exchange membrane which will trigger a series of chemical side effects, (4) the three parts above will form a cyclic process which will last until the fuel cell fails. The flow mass transfer process will further aggravate the tearing of the proton exchange membrane, resulting in new interfaces born in the proton exchange membrane, which will greatly affect its mass transfer capacity.

The above analysis indicates that static stress to the membrane electrode assembly can cause visible mechanical damage, which will combine with the internal flow mass transfer process will trigger further destruction of the internal structure and kill the fuel cell slowly.

4. Conclusions

In this paper, the destruction triggering of membrane electrode assembly was studied by transmission electron microscopy and scanning electron microscopy, the main conclusions are as follow:

- (1) The movement and agglomeration of platinum particles can directly reflect the current working state and destruction level of the fuel cell. The moving distance of platinum particles and the size of platinum particle agglomeration are positively correlated with the working time of the fuel cell.
- (2) The mechanical stress and thermal stress of the membrane electrode assembly can be divided into external stress and internal stress. External stress mainly acts at the interface between the gas diffusion layer and the proton exchange membrane and causes surface crack to both components while the components inside are basically intact. Internal stress locally destroys the inside of the component. In terms of dynamic properties, external stress is completed and stabilized in a short time due to external stress acting on the overall interface, and the internal stress generation process is related to the internal mass transfer process of the fuel cell, and belongs to a continuous dynamic process.
- (3) The flow mass transfer, mechanical damage, thermal damage and electrochemical damage in fuel cells are not independent processes, there is a logical circulation relationship: Mechanical and thermal damage play a trigger role in the ultimate destruction and failure of the membrane electrode assembly, which will affect the flow mass transfer process, the flux of the working gas in the membrane electrode assembly is abnormally increased, resulting in further component destruction and negative electrochemical reaction.
- (4) In order to extend the fuel cell life, preventing mechanical and thermal damage of membrane electrode assembly plays a vital role in designing fuel cells. Since the stress will damage the membrane electrode assembly from the external and internal way, similarly, the protection measures should also be provided from two aspects. On the one hand, the fixture should try to avoid the distribution of stress points in the area of the membrane electrode assembly on the basis of ensuring the sealing to minimize the external stress. On the other hand, the proton exchange membrane requires lower swelling rate and proper drainage measures in the off state to reduce the mechanical deformation of the membrane electrode assembly due to the temperature-dependent volume change of the moisture in the membrane.

Declaration of Competing interest

The authors declare that they have no known competing financial interests or personal relationships that could have appeared to influence the work reported in this paper.

Acknowledgements

This work was funded by the National Natural Science Foundation of China 51876161.

References

- [1] Y.Q. Tang, W.Z. Fang, H. Lin, et al., Thin film thermocouple fabrication and its application for real-time temperature measurement inside PEMFC, *Int J Heat Mass Transf* 141 (2019) 1152–1158, doi:10.1016/j.ijheatmasstransfer.2019.07.048.
- [2] T. Chen, S.H. Liu, J.W. Zhang, et al., Study on the characteristics of GDL with different PTFE content and its effect on the performance of PEMFC, *Int J Heat Mass Transf* 128 (2019) 1168–1174 <http://dx.doi.org/>, doi:10.1016/j.ijheatmasstransfer.2018.09.097.
- [3] N.T. Truc, S. Ito, K. Fushinobu, Numerical and experimental investigation on the reactant gas crossover in a PEM fuel cell, *Int J Heat Mass Transf* 127 (2018) 447–456 <http://dx.doi.org/>, doi:10.1016/j.ijheatmasstransfer.2018.07.092.
- [4] L. Chen, W.Q. Tao, Study on Diffusion Processes of Water and Proton in PEM Using Molecular Dynamics Simulation, *Materials science forum* 704–705 (PT.2) (2011) 1266–1272 <http://dx.doi.org/>, doi:10.4028/www.scientific.net/MSF.704-705.1266.
- [5] D.H. Wen, L.Z. Yin, Z.Y. Piao, et al., Performance investigation of proton exchange membrane fuel cell with intersecting flow field, *Int J Heat Mass Transf* 121 (2018) 775–787 <http://dx.doi.org/>, doi:10.1016/j.ijheatmasstransfer.2018.01.053.
- [6] Z.C. Liu, X.B. Zeng, Y. Ge, Multi-objective optimization of operating conditions and channel structure for a proton exchange membrane fuel cell, *Int J Heat Mass Transf* 111 (2017) 289–298 <http://dx.doi.org/>, doi:10.1016/j.ijheatmasstransfer.2017.03.120.
- [7] R. Borup, J. Meyers, B. Pivovar, et al., Scientific aspects of polymer electrolyte fuel cell durability and degradation, *Chem. Rev.* 107 (2007) 3904–3951 <http://dx.doi.org/>, doi:10.1002/chin.200750270.
- [8] D.A. Harvey, H.L. Tang, M. Pan, et al., Statistical simulation of the performance and degradation of a PEMFC membrane electrode assembly, *ECS Trans* 50 (2007) 147–154 <http://dx.doi.org/>, doi:10.1149/05002.0147ecst.
- [9] C. Wang, S.B. Wang, J.B. Zhang, et al., The Durability Research on the Proton Exchange Membrane Fuel Cell for Automobile Application, *Progress in Chemistry* 27 (2015) 424–435 <http://dx.doi.org/>, doi:10.7536/PC140807.
- [10] Y. Li, K. Moriyama, W. Gu, S. Arisetty, C.Y. Wang, A One-Dimensional Pt Degradation Model for Polymer Electrolyte Fuel Cells, *J Electrochem Soc* 162 (2015) F834–F842 <http://dx.doi.org/>, doi:10.1149/2.0101508jes.
- [11] P. Urchaga, T. Kadyk, S.G. Rinaldo, et al., Catalyst Degradation in Fuel Cell Electrodes: accelerated Stress Tests and Model-based Analysis, *Electrochim. Acta* 176 (2015) 1500–1510 <http://dx.doi.org/>, doi:10.1016/j.electacta.2015.03.152.
- [12] C. Robin, M. Gerard, A.A. Franco, P. Schott, Multi-scale coupling between two dynamical models for PEMFC aging prediction, *Int J Hydrogen Energy* 38 (2013) 4675–4688 <http://dx.doi.org/>, doi:10.1016/j.ijhydene.2013.01.040.
- [13] X.G. Yang, Q. Ye, P. Cheng, In-plane transport effects on hydrogen depletion and carbon corrosion induced by anode flooding in proton exchange membrane fuel cells, *Int J Heat Mass Transf* 55 (2012) 4754–4765 <http://dx.doi.org/>, doi:10.1016/j.ijheatmasstransfer.2012.04.040.
- [14] L. Chen, X. Xiang, S.Y. Wang, et al., Effects of Pt particle on structure and protons transport of Nafion membrane, *Int J Heat Mass Transf* 148 (2020) 118977.1–118977.7 <http://dx.doi.org/>, doi:10.1016/j.ijheatmasstransfer.2019.118977.
- [15] M. Zhao, W.Y. Shi, B.B. Wu, et al., Influence of Membrane Thickness on Membrane Degradation and Platinum Agglomeration under Long-term Open Circuit Voltage Conditions, *Electrochim. Acta* 153 (2015) 254–262 <http://dx.doi.org/>, doi:10.1016/j.electacta.2014.12.024.
- [16] S. Kreitmeyer, G.A. Schuler, A. Wokaun, F.N. Buechi, Investigation of membrane degradation in polymer electrolyte fuel cells using local gas permeation analysis, *J Power Sources* 212 (2012) 139–147 <http://dx.doi.org/>, doi:10.1016/j.jpowsour.2012.03.071.
- [17] B. Wu, M. Zhao, W.Y. Shi, et al., The degradation study of Nafion/PTFE composite membrane in PEM fuel cell under accelerated stress tests, *Int J Hydrogen Energy* 39 (2014) 14381–14390 <http://dx.doi.org/>, doi:10.1016/j.ijhydene.2014.02.142.
- [18] T. Uchiyama, M. Kato, T. Yoshida, Buckling deformation of polymer electrolyte membrane and membrane electrode assembly under humidity cycles, *J Power Sources* 206 (2012) 37–46 <http://dx.doi.org/>, doi:10.1016/j.jpowsour.2012.01.073.
- [19] S. Xiao, H. Zhang, The investigation of resin degradation in catalyst layer of proton exchange membrane fuel cell, *J Power Sources* 246 (2014) 858–861 <http://dx.doi.org/>, doi:10.1016/j.jpowsour.2013.07.004.
- [20] S.A. Vilekar, R. Datta, The effect of hydrogen crossover on open-circuit voltage in polymer electrolyte membrane fuel cells, *J Power Sources* 195 (2010) 2241–2247 <http://dx.doi.org/>, doi:10.1016/j.jpowsour.2009.10.023.
- [21] N.S. Khattra, Z. Lu, A.M. Karlsson, et al., Time-dependent mechanical response of a composite PFSA membrane, *J Power Sources* 228 (2013) 256–269 <http://dx.doi.org/>, doi:10.1016/j.jpowsour.2012.11.116.
- [22] V.V. Atrazhev, T.Y. Astakhova, D.V. Dmitriev, et al., The Model of Stress Distribution in, *Polymer Electrolyte Membrane, J Electrochem Soc* 160 (2013) F1129–F1137 <http://dx.doi.org/>, doi:10.1149/2.079310jes.

- [23] S. Xiao, H.M. Zhang, et al., Degradation location study of proton exchange membrane at open circuit operation, *J Power Sources* 195 (2010) 5305–5311 <http://dx.doi.org/>, doi:10.1016/j.jpowsour.2010.03.010.
- [24] H.J. Lee, M.K. Cho, Y.Y. Jo, Application of TGA techniques to analyze the compositional and structural degradation of PEMFC MEAs, *Polym. Degrad. Stab.* 97 (2012) 1010–1016 <http://dx.doi.org/>, doi:10.1016/j.polymdegradstab.2012.03.016.
- [25] T. Akita, T. Akira, M. Junko, Analytical TEM study of Pt particle deposition in the proton-exchange membrane of a membrane-electrode-assembly, *J Power Sources* 159 (2006) 461–467 <http://dx.doi.org/>, doi:10.1016/j.jpowsour.2005.10.111.
- [26] T. Shibaguchi, T. Sugiura, T. Fujitsu, T. Nomura, Y. Ohira, Effects of icing or heat stress on the induction of fibrosis and/or regeneration of injured rat soleus muscle, *Journal of Physiological Sciences* 66 (2016) 345–357 <http://dx.doi.org/>, doi:10.1007/s12576-015-0433-0.
- [27] L. Chen, Y.L. He, W.Q. Tao, The Temperature Effect on the Diffusion Processes of Water and Proton in the Proton Exchange Membrane Using Molecular Dynamics Simulation, *Numerical Heat Transfer Part a - Applications* 65 (2014) 216–228 <http://dx.doi.org/>, doi:10.1080/10407782.2013.784677.
- [28] L. Chen, P.F. Chen, Z.Z. Li, Y.L. He, W.Q. Tao, The study on interface characteristics near the metal wall by a molecular dynamics method, *Comput Fluids* 164 (2018) 64–72 <http://dx.doi.org/>, doi:10.1080/10.1016/j.compfluid.2017.03.013.